# Sum-Frequency Generation of Continuous-wave Light at 194 nm*

D.J. Berkeland, F.C. Cruz and J.C. Bergquist
*National Institute of Standards and Technology, Time and Frequency Division,*
*325 Broadway, Boulder ,CO 80303*

Over 2 mW of continuous-wave tunable 194 nm light is produced by sum-frequency mixing approximately 500 mW of 792 nm and 500 mW of 257 nm radiation in beta-barium borate (BBO). The powers in both fundamental beams are enhanced in separate ring cavities whose optical paths overlap in the Brewster-cut BBO crystal. Due to the higher circulating fundamental powers, the sum-frequency generated power is nearly two orders of magnitude greater than previously reported values.

Key words: Sum-frequency generation, second-harmonic generation, ultraviolet light, lasers, diode lasers, optical cavities

Tunable narrow-band sources of ultraviolet radiation have applications in laser-cooling and in spectroscopy of atoms and molecules. In particular, light at 194.1 nm drives the 6s 2S1/2-6p 2P1/2 resonance in singly ionized mercury. This allows laser-cooling, Raman-cooling, double-resonance experiments and other experiments on strings of electromagnetically trapped Hg+ ions [i, ii]. Because available nonlinear materials cannot be phase-matched for second-harmonic generation (SHG) to 194 nm [iii], light at this wavelength is produced by sum-frequency generation (SFG). Also, because most materials absorb in the ultraviolet, only a few crystals are suitable for generation of light in this region. Previously, several microwatts of continuous-wave 194 nm radiation have been produced by SFG in potassium pentaborate (KB5) [iv] and 31 μW in beta-barium borate (BBO) [v]. Here we report the generation of over 2 mW of coherent cw radiation at 194 nm.

Figure 1 shows an overview of the apparatus. As in Refs. iv and v, the wavelengths of the fundamental beams are 792 nm and 257 nm, where the 257 nm light is produced by frequency-doubling the 515 nm light from a single-frequency argon-ion laser. The fundamental beams are

enhanced in separate resonant cavities whose smallest waists overlap. At this intersection, the beams propagate collinearly in a Brewster-cut, angle-tuned BBO crystal to produce the sum-frequency generated 194 nm radiation.

Light at 515 nm is provided by an argon-ion laser made to run at a single frequency by a temperature-tuned intra-cavity etalon. An active servo adjusts the temperature of the etalon to maintain maximum power, which eliminates mode hops. Feedback to the position of a piezo-mounted cavity mirror stabilizes the laser frequency relative to a low-finesse reference cavity, reducing short-term fluctuations to less than 1 MHz. Long-term drift is removed by feedback to the reference cavity length so that the laser frequency maintains resonance with a hyperfine feature in molecular iodine [vi].

The 515 nm beam is mode matched into a power enhancement cavity in which a 3×3×5 mm, angle-tuned, Brewster-cut BBO crystal is placed. The cavity consists of two 10 cm radius of curvature mirrors, a 30 cm radius of curvature mirror and a flat input coupler that transmits 1.8% of the input power. The round-trip length of the cavity is 1.35 m, and the 28 μm minimum beam waist is between the two 10 cm mirrors. The crystal is heat sunk by pressing it into a slot in an aluminum block. Thin indium foil is placed between the crystal and the aluminum to ensure good thermal contact. The crystal is placed at the 28 μm waist so that the fundamental beam propagates as an o-wave for type-I phase matching. A dichroic beam splitter reflects 97% of the harmonically generated 257 nm light while transmitting the 515 nm light. The cavity is locked to resonance with the incident radiation using the Hänsch-Couillaud method [vii], as are all other cavities in this experiment. With the crystal in place and at low circulating powers, the power enhancement factor is 120.

However, with an incident power of 2 W, the enhancement is reduced to roughly 90 because of nonlinear conversion loss. As the circulating power increases, fractionally more of the fundamental power is transferred to the second-harmonic beam. This increases the cavity losses, lowering the power enhancement factor. Consequently, the overall conversion efficiency $\varepsilon = P_{257}/P_{515}$, where $P_{515}$ is the input power at 515 nm and $P_{257}$ is the output power at 257 nm, does not increase linearly with the input power. Rather, it is determined by [viii,ix]

$$\sqrt{\varepsilon} = \frac{4T\sqrt{\eta P_{515}}}{\left[2 - \sqrt{1-T}\left(2 - L - \sqrt{\varepsilon\,\eta\,P_{515}}\right)\right]^2}, \tag{1}$$

where $T$ is the transmission of the input coupler, $L$ is round-trip loss not including conversion losses, and $\eta$ is the single-pass efficiency of the crystal measured at low powers. Figure 2 shows the theoretically expected values of $\varepsilon$ as a function of input power, along with our measured values of $\varepsilon$, corrected by the Fresnel loss of the second harmonic beam at the exit face of the crystal. For 5.6 W of input power we obtain 2.0 W of second harmonic radiation. The measured efficiencies, however, are significantly lower than the theoretical values for input powers of 2 W and greater.

This discrepancy is explained by the small, but finite, absorption of the harmonically generated UV light. As more 257 nm radiation is generated, the crystal develops an anisotropic temperature gradient due to the non-uniform intensity distribution of the harmonic power. Since the indices of refraction are temperature dependent, a thermal lens is created in the crystal. This changes the mode-matching efficiency between the input beam and the cavity, which decreases the circulating power [x]. The resulting feedback between the intra-cavity power and the thermal lens can in turn destabilize the cavity resonance [viii]. The heat sink controls the crystal temperature sufficiently that the cavity can be tightly locked with at least 6 W of input power.

However, because the heat sink does not eliminate the thermal lens, our optimum conversion efficiency is limited to 40%.

Approximately 500 mW of 257 nm radiation is mode matched into a second power enhancement cavity containing a second, angle-tuned BBO crystal used for SFG to 194 nm. Because the 257 nm radiation is generated in angle-tuned BBO, its beam profile at the crystal surface is approximately rectangular along the walk-off direction [viii, xi]. The beam's width is the walk-off distance $\rho\,\ell$, where $\rho$ is the walk-off angle and $\ell$ is the length of the crystal. Since the overlap of this beam profile with a Gaussian distribution of width $w_0 = \frac{1}{2}\,\rho\,\ell$ is [xii]

$$\xi = \left[ \int_{-w_0}^{w_0} \left( \frac{2}{\pi\, w_0} \right)^{1/4} \exp\left[ -\frac{x^2}{w_0^2} \right] \sqrt{\frac{1}{2\, w_0}}\, dx \right]^2 = 0.89\,, \qquad (2)$$

the second harmonic beam can be mode-matched with up to $\xi$ = 89% efficiency Into a cavity with spherically symmetric Gaussian modes. After passing through suitably chosen spherical and elliptical mode-matching lenses, approximately 85% of the input beam is coupled into the enhancement cavity's $TEM_{00}$ mode.

The 257 nm power enhancement cavity is formed by two 30 cm radius of curvature mirrors and two flat mirrors, which includes a 9% transmitting input coupler. The round-trip length is 1.79 m, and the minimum waist, located midway between the two curved mirrors, is 39 μm wide. The power enhancement factor of the empty cavity is about 27. When the Brewster-cut BBO crystal is positioned at the cavity waist so that it is near Brewster's angle, the build-up factor can be as great as 21. Due to gradual UV-induced degradation of the cavity surfaces, the build-up factor at the time of this measurement is roughly 12. With 500 mW input, then, the circulating 257 nm power is 6 W.

As in the SHG cavity, the high power and intensity of the circulating 257 nm radiation (> 240 $kW \cdot cm^{-2}$ for 6 W circulating power) has several adverse effects on the 257 nm enhancement cavity. Thermal lensing in the SFG BBO crystal destabilizes the intracavity power as explained above. The baseline of the Hänsch-Couillaud dispersion signal also drifts significantly. This may be due to the increased intensity of reflected higher-order cavity modes combined with slight beam misalignments. It is also possible that changes in the crystal birefringence slightly alter the polarization of the light reflected from the cavity. Changes in the crystal's indices of refraction also alter the phase-matching conditions for SFG. Thus, the difference in the 194 nm beam position when the cavity is locked into resonance versus when it is swept through resonance is roughly 3 mrad. The beam also moves as the crystal temperature fluctuates over the course of the day. These problems are greatly reduced when the SFG crystal is heat sunk in the same way as the SHG crystal, although the 257 nm intra-cavity power can still vary by more than 10% over tens of minutes.

Approximately 500 mW of narrow-band single-frequency radiation at 792 nm is produced by a master-oscillator-power-amplifier (MOPA) system [xiii]. The master laser is an external cavity diode laser in the Littman configuration, whose free-running line width is less than 0.5 MHz. The frequency of the master laser is stabilized to an external cavity whose length is servoed to light from the iodine-stabilized argon-ion laser. About 18 mW from the master laser are mode-matched into a tapered amplifier [xiv] acting as a slave laser. With no more than 1.1 A into the slave laser, up to 600 mW can be safely generated. We have verified that the frequency of the slave laser is phase locked to the master laser with as little as 3 mW of injected power. The shape of the slave laser beam is transformed so that it is nearly spherically Gaussian, after which the beam is mode-matched into a power enhancement cavity with greater than 90% efficiency.

The 792 nm enhancement cavity is formed by two 30 cm radius of curvature mirrors and two flat mirrors. The round-trip length of the cavity is 1.83 m, and the minimum cavity waist size is approximately 68 μm. The transmission of the input coupler is 1.5% and the build-up factor of the empty cavity is about 80. With the crystal placed near the cavity waist so that its surfaces are at Brewster's angle, the power enhancement is reduced only slightly. Thus for 600 mW input power, the circulating power is 48 W. Aside from a 10% decrease in intracavity power when the 257 nm cavity is locked to resonance, the 792 nm cavity is not affected by thermal lensing in the crystal at these powers.

The 792 nm and 257 nm cavities are situated so that the intra-cavity beams coincide at the crystal position near the minimum beam waists. The Brewster-cut SFG BBO crystal is 4×4×5.75 mm, and cut at 71.6° to the optic axis. Both fundamental beams propagate as o-waves inside the crystal, while the SFG beam propagates as an e-wave. To make the beams collinear inside the crystal, the incidence angles of the fundamental beams at the crystal are adjusted to account for the difference in refraction angles. Only the 792 nm beam is strictly at Brewster's angle. Because of the differences in refraction angles of the SFG and fundamental beams, the 194 nm beam is sufficiently separated from the 792 nm and 257 nm beams to pass the cavity optics easily. For the conditions described here, a NIST calibrated photodiode measures 1.4 mW of 194 nm radiation 2.0 m from the crystal. If absorption in air and the Fresnel loss at the exit surface of the crystal are accounted for, about 2.2 mW of radiation is generated.

To conclude, we have produced more than 2 mW of 194 nm radiation, which is two orders of magnitude greater than previously reported. This is partly due to production of 500 mW of 257 nm radiation by SHG in BBO, whereas previous experiments produced only 20 to 30 mW by SHG in ammonium dihydrogen phosphate (ADP) [iv, v]. Further, although the quality

of the 257 nm power enhancement cavity is not improved over that reported in Ref. v, the build-up factor of the 792 nm power enhancement cavity is seven times that of Refs. iv and v. The 194 nm power may still be increased by about a factor of 3 by decreasing the intra-cavity beam waist sizes to closer to the optimum size of about 15 μm [xi], and by increasing the build-up factor of the 257 nm power enhancement cavity. However, the higher intensities (especially at 257 nm) might cause crystal damage or severe thermal problems.

We would like to thank S. Mioc, D. Meekhof, M. Young and D. Sullivan for careful reading of this manuscript. F.C. Cruz acknowledges the support of CAPES (Brazil).

Figure 1: Optical layout. DBS: dichroic beam splitter; EL: elliptical lens; PD: photodiode. Not shown are optics and electronics for stabilizing and analyzing laser frequencies or for stabilizing enhancement cavities.

Figure 2: Theoretically expected values of SHG efficiency from equation 1 (solid line) and measured values (dots). Calculated values use $\eta$ = 6.0 $10^{-5}$ $W^{-1}$, $L$ = 0.007 m, and $T$ = 0.015.

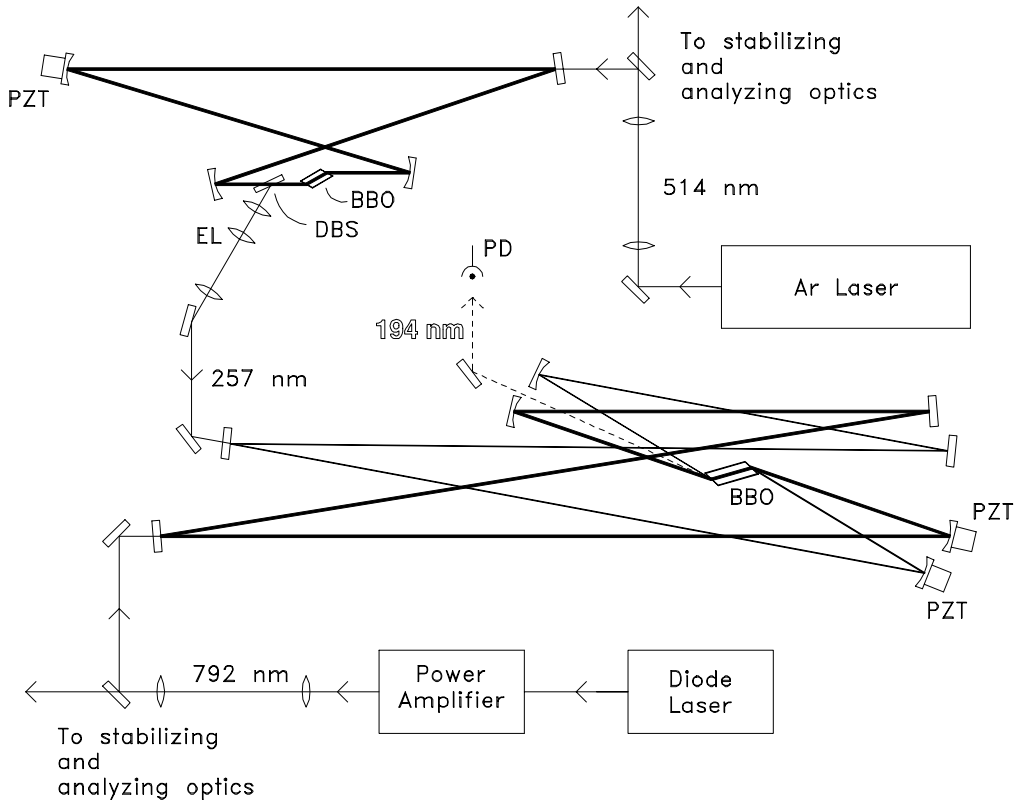


Figure 1: Optical layout. DBS: dichroic beam splitter; EL: elliptical lens; PD: photodiode. Not shown are optics and electronics for stabilizing and analyzing laser frequencies or for stabilizing enhancement cavities.

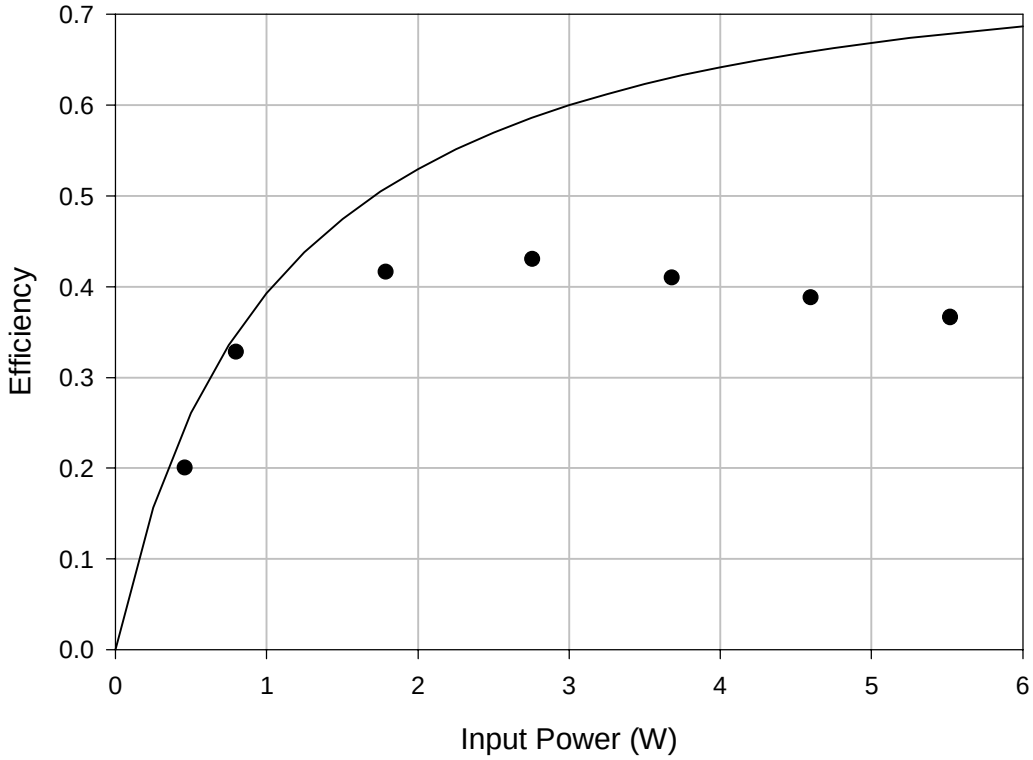


Figure 2: Theoretically expected values of SHG efficiency from equation 1 (solid line) and measured values (dots). Calculated values use $\eta$ = 6.0 $10^{-5}$ $W^{-1}$, $L$ = 0.007 m, and $T$ = 0.015.

[i] M.G. Raizen, J.M. Gilligan, J.C. Bergquist, W.M. Itano, and D.J. Wineland, "Ionic crystals in a linear Paul trap," Phys. Rev. A **45**, 6493 (1992).

[ii] John Miller, Dana Berkeland, Flavio Cruz, Jim Bergquist, Wayne Itano and Dave Wineland, "Cryogenic linear trap for accurate spectroscopy," in Proceedings of the 1996 IEEE International Frequency Control Symposium, Honolulu, HI, 1996, to be published.

[iii] The crystal $Sr_2Be_2B_2O_7$ (SBBO) has produced wavelengths as short as 177.3 nm by SHG: Chuangtian Chen, Baichang Wu, Wenlong Zeng, Yebin Wang, Ning Ye, Linhua Yu, "New nonlinear optical crystal $Sr_2Be_2B_2O_7$: Growth and properties," QELS, 1996 Technical Digest Series, Anaheim, CA, June 2-7, 1996 (unpublished, paper JTuI2). The crystal $KBe_2BO_3F_2$ (KBBF) has produced 184.7 nm SHG output: Chuangtian Chen, Zuyan Xu, Daoqun Deng, J. Zhang, G.K.L. Wong, Baichang Wu, Ning Ye, and Dingyan Tang, "The vacuum ultraviolet phase-matching characteristics of nonlinear optical $KBe_2BO_3F_2$ crystal," Appl. Phys. Lett. **68**, 2930 (1996).

[iv] H. Hemmati, J.C. Bergquist, and Wayne M. Itano, "Generation of continuous-wave 194-nm radiation by sum-frequency mixing in an external ring cavity," Opt. Lett. **8**, 73 (1983).

[v] M. Watanabe, K. Hayasaka, H. Imago and S. Urabe, "Continuous-wave sun-frequency generation near 194 nm with a collinear double enhancement cavity," Opt. Comm. **97**, 225 (1993).

[vi] J.C. Bergquist, H. Hemmati, and W.M. Itano, "High power second harmonic generation of 257 nm radiation in an external ring cavity," Opt. Comm. **43**, 437 (1982).

[vii] T.W. Hänsch and B. Couillaud, "Laser frequency stabilization by polarization spectroscopy of a reflecting reference cavity," Opt. Comm. **35**, 441 (1980).

[viii] A. Steinbach, M. Rauner, F.C. Cruz, and J.C. Bergquist, "CW second harmonic generation with elliptical Gaussian beams," Opt. Comm. **123**, 207 (1996).

[ix] W.J. Kolowsky, C.D. Nabors and R.L. Byer, "Efficient second harmonic generation of a diode-laser-pumped CW Nd:YAG laser using monolithic MgO:$LiNbO_3$ external resonant cavities," IEEE J. Quantum Electron. **24**, 913 (1988).

[x] E.S. Polzik and H.J. Kimble, "Frequency doubling with $KNbO_3$ in an external cavity," Opt. Lett. **16**, 1400 (1991).

[xi] G.D. Boyd and D.A. Kleinman, "Parametric interaction of focused Gaussian light beams," J. Appl. Phys. **39**, 3597(1968).

[xii] M.G. Boshier, "Precise laser spectroscopy of the hydrogen 1S-2S transition," D. Phil. Thesis, University of Oxford, 1988.

[xiii] F.C. Cruz, M. Rauner, J.H. Marquardt, L. Hollberg, and J.C. Bergquist, "An all solid-state $Hg^+$ optical frequency standard," Proceedings of the Fifth Symposium on Frequency Standards and Metrology, James C. Bergquist, Ed. (World Scientific, 1996), pp. 511-513.

[xiv] SDL-8630; The mention of brand names in this paper is for information purposes only and does not constitute an endorsement of the product by the authors or their institutions.